



Investigation of pressure-induced phase transitions of the solar cell materials $\text{CdSe}_{1-x}\text{Te}_x$ alloys: one- and two-dimensional search DFT calculation

A. H. Reshak & M. Jamal

To cite this article: A. H. Reshak & M. Jamal (2017): Investigation of pressure-induced phase transitions of the solar cell materials $\text{CdSe}_{1-x}\text{Te}_x$ alloys: one- and two-dimensional search DFT calculation, Phase Transitions

To link to this article: <http://dx.doi.org/10.1080/01411594.2017.1326600>



Published online: 17 May 2017.



Submit your article to this journal [↗](#)



View related articles [↗](#)



View Crossmark data [↗](#)

RESEARCH ARTICLE



Investigation of pressure-induced phase transitions of the solar cell materials $\text{CdSe}_{1-x}\text{Te}_x$ alloys: one- and two-dimensional search DFT calculation

A. H. Reshak^{a,b} and M. Jamal^c

^aNew Technologies – Research Center, University of West Bohemia, Pilsen, Czech Republic; ^bSchool of Material Engineering, Universiti Malaysia Perlis, Kangar, Malaysia; ^cYoung Researchers and Elite Club, Islamshahr Branch, Islamic Azad University, Tehran, Iran

ABSTRACT

Gibbs script within the all-electron full potential linearized augmented plane wave (FP-LAPW) method has been used to calculate pressure-induced phase transition at zero temperature for selected phases. The calculation exhibits that CdSe is stable at wurtzite phase whereas $\text{CdSe}_{0.75}\text{Te}_{0.25}$, $\text{CdSe}_{0.5}\text{Te}_{0.5}$, $\text{CdSe}_{0.25}\text{Te}_{0.75}$ and CdTe are stable at cubic phase. This prediction is consistent with experimental work of Schenk and Silber at $T < 800^\circ\text{C}$ except for $\text{CdSe}_{0.75}\text{Te}_{0.25}$. We found that increasing the Te content for both phases of ternary $\text{CdSe}_{1-x}\text{Te}_x$ alloys decreases the optimized energy and bulk modulus, hence leads to decrease hardness, while it increases the optimized volume. The density functional theory (DFT) calculation within generalized gradient approximation (PBE-GGA) and the two-dimensional search of equation of state for wurtzite phase predict a possible pressure-induced phase transition from cubic to wurtzite phase for the ternary $\text{CdSe}_{0.5}\text{Te}_{0.5}$, $\text{CdSe}_{0.75}\text{Te}_{0.25}$ and CdTe at pressures of about 13.6, 1.9 and 10.6 (GPa) with corresponding volume collapses at the phase-transition boundary of about 181.115 and 180.525, 203.839 and 203.485 and 203.337 and 202.692 ($\text{bohr}^3/\text{atom}$), respectively. However, one-dimensional search of equation of state for wurtzite phases predicts a possible pressure-induced phase transition at pressures 14.5, 1.9 and 11.4 for $\text{CdSe}_{0.5}\text{Te}_{0.5}$, $\text{CdSe}_{0.75}\text{Te}_{0.25}$ and CdTe, respectively.

ARTICLE HISTORY

Received 25 October 2016
Accepted 25 April 2017

KEYWORDS

Electronic materials;
inorganic compounds;
optical materials;
semiconductors; crystal
structure

PACS

71.15.Mb; 71.20.-b

1. Introduction

From past to present years, binary and ternary cadmium chalcogenides have attracted special attention for their applications in γ -ray detectors, infrared windows, solar cells and other optoelectronic devices [1–12]. Several researches have extensively investigated the structural, electronic, optical and thermodynamic properties of cadmium chalcogenides [7,10–13]. However, very few new theoretical results on $\text{CdSe}_{1-x}\text{Te}_x/\text{CdSe}_x\text{Te}_{1-x}$ alloys [14–16] are reported. Ternary cadmium-selenide-telluride is a promising candidate for numerous applications [16,17,12], especially for a photovoltaic cell for which the ideal band gap is 1.4 eV [17]. The effect of various tellurium contents plays a principal role in fabricating novel materials with adjustable structural, electronic, optical and magnetic properties. Researchers have, therefore, found that the band gap of $\text{CdSe}_x\text{Te}_{1-x}$ thin film is between 1.3 and 1.7 eV. This band gap can be adjusted by changing the x value to gain the ideal band gap (1.4 eV) for solar cell applications [17].

The principal requirements for a good thin film photoelectrode to design high-efficiency photoelectrochemical cells using $\text{CdSe}_{1-x}\text{Te}_x$ alloys were extensively investigated [18]. Several researchers have studied thin film of cadmium chalcogenide extensively [12] using different techniques such as glassy system [8], electrodeposition method [19] and molecular beam epitaxial [20]. Ravichandran et al. [21], by using the electro-deposition method with varying doping concentrations of Te, studied the photoconductivity of $\text{CdSe}_{1-x}\text{Te}_x$ thin films at room temperature as a function of applied dc-electric field, wavelength and intensity of incident light. They established that increasing the Te content leads to decreasing the energy band gap of $\text{CdSe}_{1-x}\text{Te}_x$. Muthukumarasamy et al. [22] have investigated the structural phase transformation and optical band gap bowing in hot wall-deposited $\text{CdSe}_x\text{Te}_{1-x}$ thin films. They reported the band gap of 1.45 eV for $\text{CdSe}_{0.6}\text{Te}_{0.4}$ thin film which is very close to the ideal band gap (1.4 eV) for solar cell applications. A density functional theory (DFT) investigation was carried out for $\text{CdS}_{1-x}\text{Se}_x$ and $\text{CdS}_{1-x}\text{Te}_x$ alloys with x vary between 0.0 and 1.0 (step of 0.5), resulting in an energy band gap reduction when one moves from 0.0 to 1.0 [23]. Since $\text{CdSe}_{1-x}\text{Te}_x$ is a ternary alloy consisting of CdSe (wurtzite structure) and CdTe with zinc-blende structure, it is expected a phase transition in the crystal structure of $\text{CdSe}_{1-x}\text{Te}_x$ occurs when we vary Se or Te composition. This behavior motivates several researcher to study the structural phase transformation of this ternary alloys for different values of Se or Te composition. Schenk and Silber [24] found that there are two phases for $\text{CdSe}_x\text{Te}_{1-x}$ alloys. The first one is cubic in the composition range of $0 \leq X_{\text{CdSe}} \leq 0.45$ and the second one is hexagonal phase in the range of $0.65 \leq X_{\text{CdSe}} \leq 1.0$. Uthanna and Jayarama Reddy [25], Mangalhari et al. [26] and Islam et al. [27] found that $\text{CdSe}_x\text{Te}_{1-x}$ ($0 \leq x \leq 1$) ternary thin films, independent of composition, are zinc-blende (cubic phase). The new work of Shinde et al. [11] revealed that $\text{CdSe}_{0.6}\text{Te}_{0.4}$ thin films exhibit hexagonal crystal structure in nature, using X-ray diffraction study. Recently, Reshak et al. [17] studied the lattice parameters and ground state of bulk $\text{CdSe}_{1-x}\text{Te}_x$ alloys with increasing Te content for two phases, i.e. cubic and hexagonal by using one-dimensional (1D) search of equation of state (EOS) for hexagonal phase, i.e. changes in the volume at constant c/a ratio which may play as a source of error because hexagonal phases have two degrees of freedom (changes in the volume and c/a ratio) for finding EOS. On the other hand, there are very few studies [28–35] on the structural phase transition in ternary semiconductor alloys. The above works motivated us to put two questions: (1) ‘what is the pressure of phase-induced transition for $\text{CdSe}_{1-x}\text{Te}_x$ ternary alloys from hexagonal to cubic phase?’, (2) ‘which phase is the most stable?’, and try to answer them. We hope that, our results provide a useful reference for future experimental works and theoretical studies. In the phase transition, the crossover from a small gap semiconductor to a metallic state could occur such as in the case of $\text{ZnSe}_x\text{Te}_{1-x}$ alloys [34]. To answer these questions, our goal can be formulated as follows: (1) we studied the ground-state properties and the pressure of phase-induced transition for two phases of bulk $\text{CdSe}_{1-x}\text{Te}_x$ ternary alloys with increasing Te content at 0 K excluding the effects of temperature, substrate, etc., and our results were compared with available experimental data, (2) we used the full potential linear augmented plane wave plus local orbital (FP-LAPW+lo) [36–38] method using two-dimensional search of EOS (not 1D-search of EOS) for finding EOS for hexagonal phase using 2Doptimize package [39]. The effect of 2D-search of EOS is found to be important for accurate results [40]. The FP-LAPW+lo has proven to be one of the accurate methods for the computation of the electronic structure of solids within DFT [41–44]. The organization of this article is as follows. In Section 1, we briefly describe introduction. Section 2 contains the method of calculations and computational details. In Section 3, we provide our results (structural properties and phase transition as stable phase) and compare them with available theoretical and experimental data. Finally, in Section 4, our conclusion is given.

2. Method of calculations

The basic method to calculate pressure-induced phase transition at zero temperature ($T = 0$) is to calculate difference of Gibbs-free-energy for selected phases at the same pressure grid. As

$G = E + PV - TS$ at $T \neq 0$, therefore, $G = E + PV$ at $T = 0$. That means we have to calculate the energy (E) and volume (V) at any pressure (P) for the two phases. For this purpose, at the first step, we evaluate the equation of state using Murnaghan equation (see the following equation) by using the calculated total energy as a function of volume changes (1D-search) for cubic phase, while for the hexagonal phase, the calculated total energy as a function of volume and c/a changes (2D-search) is used.

$$E(V) = E_o + \frac{BV}{B'} \left\{ 1 + \frac{1}{B' - 1} \left(\frac{V_o}{V} \right)^{B'} \right\} - \frac{BV_o}{B' - 1}.$$

Using the parameters obtained (E_o – optimized energy, V_o – optimized volume, B – bulk modulus, B' – derivative of bulk modulus) from the Murnaghan equation, we can find the volume and energy at the selected pressure and hence the Gibbs-free-energy can be obtained.

$$V(P) = V_o \left\{ 1 + P \left(\frac{B'}{B} \right) \right\}^{\frac{-1}{B'}},$$

$$E(P) = E_o + \frac{BV(P)}{B'} \left\{ 1 + \frac{1}{B' - 1} \left(\frac{V_o}{V(P)} \right)^{B'} \right\} - \frac{BV_o}{B' - 1}.$$

Therefore, we can calculate the difference of Gibbs-free-energy (ΔG) for both phases on the same pressure grid. These calculations were performed using 2DRoptimize package [39] and Gibbs script within WIEN2k package [38]. More details about two-dimensional search of EOS for hexagonal compounds are available in our previous works [40,43]. The WIEN2k is an *ab initio* full potential linearized augmented plane wave (FP-LAPW) plus local orbital method for calculating the electronic and structural properties of materials based on DFT. In this procedure, the unit cell volume is divided into the non-overlapping atomic spheres around each atom with Muffin-tin radius (R_{mt}) and the remaining is the interstitial area. In the atomic spheres, the wave-functions are expanded into atomic orbitals and the maximum angular momentum of this basis function is set to $l_{\max} = 10$, while in the interstitial region, a plane-wave basis set is used and the convergence of this basis set is checked by a cutoff parameter $R_{mt}K_{\max} = 9$, where R_{mt} is the smallest atomic sphere radius in the unit cell. For these calculations, we have used 2000 k -points in the full Brillouin zone. Optimizing the atomic positions is done until forces drop at about 1 (mRy/bohr) during calculations. To treat the exchange-correlation functional, we have used the Perdew-Burke-Ernzerhof parametrization of the generalized gradient approximation (PBE-GGA) [45]. We would like to highlight that using the new package 2DRoptimize, the switches 7 or 8 and 5 in the WIEN2k package have been used for the volume and c/a changes, respectively. This means that for finding EOS for hexagonal phase, we have done at least 35 or 40 self-consistent calculations. For modeling the $\text{CdSe}_{1-x}\text{Te}_x$ ($x = 0.0, 0.25, 0.5, 0.75, 1.0$) alloys, we have used the ‘special quasirandom structures’ (SQS) approach of Zunger et al. [46] to reproduce the randomness of the alloys for the first few shells around a given site. This approach is reasonably sufficient to describe the alloys with respect to many physical properties that are not affected by the errors introduced using the concept of the periodicity beyond the first few shells. Therefore, for modeling the atomic positions for different compositions ($x = 0.25, 0.5, 0.75$) for both phases, we have started from CdSe structure. Then, using supercell method (for hexagonal phase, we made a $1 \times 1 \times 2$ supercell) or changing (for cubic phase), if symmetry permits, lattice type of our structure into P-type (primitive) conventional supercell, which allows to increase the number of atoms in this supercell (i.e. P-type) and replacing Se atom by Te atom, we could model different compositions. In Table 1, we have listed the atomic position of different compositions along with space group number.

Table 1. All of atomic positions of nonequivalent atoms as fraction of unit cell parameters for different compositions.

Atomic positions	Space group number	Compounds
Cd(1/3,2/3,0,5)	186	CdSe
Se(1/3,2/3,0,875)		
Cd1(0,0,0,8125)		
Cd2(1/3,2/3,0,5625)		
Cd3(0,0,0,3125)	156	CdSe _{0.75} Te _{0.25}
Cd4(1/3,2/3,0,0625)		
Te(0,0,0)		
Se1(0,0,0,5)		
Se2(1/3,2/3,0,75)	156	CdSe _{0.5} Te _{0.5}
Se3(1/3,2/3,0,25)		
Cd1(0,0,0,625)		
Cd2(1/3,2/3,0,125)		
Se(0,0,0)	156	CdSe _{0.25} Te _{0.75}
Te(1/3,2/3,0,5)		
Cd1(0,0,0,8125)		
Cd2(1/3,2/3,0,5625)		
Cd3(0,0,0,3125)	186	CdTe
Cd4(1/3,2/3,0,0625)		
Se(0,0,0)		
Te1(0,0,0,5)		
Te2(1/3,2/3,0,75)	216	CdSe
Te3(1/3,2/3,0,25)		
Cd(1/3,2/3,0,5)		
Te(1/3,2/3,0,875)		
Cd(0,0,0)	215	CdSe _{0.75} Te _{0.25}
Se(0.25,0.25,0.25)		
Cd(0.75,0.25,0.25)		
Te(0,0,0)		
Se(0,0,5,0.5)	1	CdSe _{0.5} Te _{0.5}
Cd1(0,0,0)		
Cd2(0.5,0.5,0)		
Cd3(0.5,0,0.5)		
Cd4(0,0.5,0.5)	215	CdSe _{0.25} Te _{0.75}
Te1(0.75,0.75,0.25)		
Te2(0.25,0.75,0.75)		
Se1(0.25,0.25,0.25)		
Se2(0.75,0.25,0.75)	216	CdTe
Cd(0.75,0.25,0.25)		
Te(0,0,5,0.5)		
Se(0,0,0)		
Cd(0,0,0)		
Te(0.25,0.25,0.25)		

Bold and non-bold fonts are for cubic and hexagonal phases, respectively.

3. Results and discussion

3.1. Structural properties

Our goal is to calculate the difference ($\Delta G = 0$) of Gibbs-free-energy ($G = E + PV$) for selected phases at the same pressure grid in order to obtain the pressure-induced phase transition at zero temperature ($T = 0$) using the calculated total energy and volume at the same pressure grid using the parameters (E_0 , V_0 , B , B') obtained from the Murnaghan equation by 1D-search (volume changes) and 2D-search (volume and c/a changes) of EOS for cubic and hexagonal phases, respectively. Therefore, at the first step, we need to investigate the ground-state properties of CdSe_{1-x}Te_x ($x = 0.0, 0.25, 0.5, 0.75, 1.0$) ternary alloys in the cubic and hexagonal phases. To make a meaningful comparison, these results along with the theoretical and experimental data are listed in Table 2. But before the discussion about the ground-state properties of CdSe_{1-x}Te_x ternary alloys, we would like to highlight that in the calculation of EOS for hexagonal compounds using 1D-search (changes the

Table 2. The calculated lattice parameters (a and c in Angstrom), bulk modulus (B in GPa), derivate of bulk modulus (B'), optimized energy (E in Ryd/atom) and optimized volume (V in bohr³/atom) for zinc-blende and wurtzite phases of CdSe_{1-x}Te_x ($x = 0.0, 0.25, 0.5, 0.75, 1.0$) alloys in comparison with available experimental and theoretical data.

Compounds	a (Å)	c (Å)	B (GPa)	B'	E (Ryd/atom)	V (bohr ³ /atom)
CdSe_{cubic}	6.208		45.62	4.37	-8026.3071	201.8622
Theo	6.207 [17], 6.210 [52], 6.050 [53], 6.216 [15]		45.60 [17], 65.12 [53], 45.16 [15]			
Exp	6.084 [47,48], 6.050 [49]		53.00 [49]			
CdSe_{wurtzite(2D)}	4.39	7.17	44.83	4.36	-8026.3073	201.6798
Theo	4.34 [17]	7.27 [17]	43.64 [17]			
Exp	4.30 [24,51]	7.02 [24], 7.01 [51]				
CdSe_{0.75}Te_{0.25} cubic	6.316		40.99	4.60	-9117.9538	212.5852
Theo	6.526 [17]		43.08 [17]			
CdSe_{0.75}Te_{0.25} wurtzite(2D)	4.463	14.579	41.21	4.59	-9117.9537	212.1766
Theo	4.429 [17]	14.891 [17]	42.32 [17]			
CdSe_{0.5}Te_{0.5} cubic	6.421		38.85	4.54	-10209.6011	223.3526
Theo	6.407 [17]		42.21 [17]			
CdSe_{0.5}Te_{0.5} wurtzite(2D)	4.536	7.421	39.06	4.35	-10209.6008	223.1363
Theo	4.437 [17]	7.459 [17]	39.14 [17]			
CdSe_{0.25}Te_{0.75} cubic	6.524		37.62	4.20	-11301.2489	234.2496
Theo	6.322 [17]		40.14 [17]			
CdSe_{0.25}Te_{0.75}wurtzite(2D)	4.610	15.088	36.59	4.42	-11301.2485	234.3089
Theo	4.563 [17]	14.653 [17]	36.31 [17]			
CdTe_{cubic}	6.629		35.45	4.51	-12392.8972	245.7054
Theo	6.620 [17], 6.626 [52], 6.480 [53], 6.631 [15], 6.540 [50]		36.24 [17], 44.50 [54], 48.94 [53], 33.78 [15]			
Exp	6.480 [47,49], 6.540 [48], 6.477 [50]		44.50			
CdTe_{wurtzite(2D)}	4.680	7.675	35.25	4.36	-12392.8969	245.6107
Theo	4.680 [17], 4.560 [50]	7.650 [17], 7.540 [50]	34.62 [17]			
Exp	4.570 [50]	7.470 [50]				

volume at constant c/a ratio), we have to use the same c/a ratio for all of volume changes. However, in the 2D-search of EOS, usually it finds the best value of c/a ratio for each value of volume changes.

To show this effect, we have calculated the best value of c/a ratio for different values of volume changes using 2DRoptimize package for wurtzite CdTe compound (see Table 3). As can be seen, this effect could be important and may play as a source of error; however, in some cases, this error may be negligible.

Our results show that for zinc-blende CdTe ($x = 1$) and CdSe ($x = 0$), the calculated a -lattice constant using PBE-GGA exchange correlation is overestimated with respect to the experiment [42–50]. However, it is observed that our results come to the same conclusions as the previous theoretical DFT-PBE calculations [17]. Usually, local density approximation (LDA) and WC-GGA underestimate lattice parameters and PBE overestimate them [40]. One can conclude that the other functionals such as LDA and WC-GGA can describe the structural parameters of CdSe and CdTe better

Table 3. The effect of 1D and 2D-search of EOS on c/a ratio of wurtzite CdTe compound for different percent of volume changes within PBE-GGA.

Volume changes of CdTe in percent	-15	-10	-5	0	5	10	15
$(c/a)_{1D\text{-search}}$	1.6430	1.6430	1.6430	1.6430	1.6430	1.6430	1.6430
$(c/a)_{2D\text{-search}}$	1.6779	1.6557	1.6482	1.6430	1.6409	1.6393	1.6379

than PBE-GGA with respect to the experimental data. For $x = 0.5$ and $x = 0.75$, our PBE-GGA a -lattice constant is bigger than that calculated by Reshak et al. [17] while for $x = 0.25$ it is smaller. However, we used the same method (FP-LAPW), but we considered more k -points (2000 k -points) in the full Brillouin zone and selected $l_{\max} = 10$, whilst in [17] they have used 1400 k -points and $l_{\max} = 6$. This can be considered the main reason for the disagreement.

Table 2 reveals that the structural parameters, namely a -lattice constant, the optimized volume, the optimized energy and resistance against the volume changes (bulk modulus) for zinc-blende CdSe $_{1-x}$ Te $_x$ within PBE-GGA functional increase, increase, decrease and decrease monotonically when we move from zinc-blende-CdSe to zinc-blende-CdTe, respectively. This is not the case for bulk modulus derivative where the alteration is non-monotonic. For wurtzite CdTe ($x = 1$) and CdSe ($x = 0$), our evaluated a and c lattice constants within PBE-GGA functional are overestimated with respect to the experiment [24,50,51]. However, one can see that our findings are in agreement with the previous [17,50] DFT-PBE or DFT-GGA calculations. For $x = 0.25$ and $x = 0.5$, our calculated a -lattice (c -lattice) constants are within PBE-GGA which are bigger (smaller) than that evaluated by Reshak et al. [17], while for $x = 0.75$, we got bigger a -lattice (c -lattice) constants than that calculated previously [17]. However, the disharmony is ascribed to the difference in the value of l_{\max} , k -points, and the method of search for finding EOS; in the previous calculations [17], they have used 1D-search, while in the present work we have used the 2D-search. Table 2 reveals the structural parameters, namely the a -lattice constant, the optimized volume, the optimized energy and resistance against the volume changes (bulk modulus) for wurtzite CdSe $_{1-x}$ Te $_x$ ($x = 0, 0.25, 0.5, 0.75, 1$). These parameters increase, increase, decrease and decrease monotonically within PBE-GGA functional when moving from wurtzite-CdSe to wurtzite-CdTe, respectively. This is not the case for bulk modulus derivative where the alteration is non-monotonic. Since the bulk modulus is related to the resistance against the volume changes, we can derive that increasing the Te content in ternary CdSe $_{1-x}$ Te $_x$ alloys led to the decrease in hardness for both phases. The polynomial fit of our calculated data regarding the bulk modulus, a -lattice constant, optimized volume and the optimized energy of ternary CdSe $_{1-x}$ Te $_x$ alloys with respect to the Te content using PBE-GGA functional for both phases leads to the following analytical expressions:

$$\begin{aligned}
B_c &= 45.281 - 16.147X + 6.663X^2, \\
B_w &= 44.750 - 14.358X + 4.846X^2, \\
a_c &= 6.208 + 0.429X - 0.009X^2, \\
a_w &= 4.390 + 0.297X - 0.006X^2, \\
V_c &= 201.909 + 41.917X + 1.823X^2, \\
V_w &= 201.644 + 41.914X + 2.083X^2, \\
E_c &= -8026.307 - 4366.586X - 0.004X^2, \\
E_w &= -8026.307 - 4366.584X - 0.005X^2,
\end{aligned}$$

Where B represents the bulk modulus for cubic (C) and wurtzite (W) phases in units of (GPa), a displays a -lattice constant in units of angstrom, V represents the optimized volume in units of (bohr³/atom) and E exhibits the optimized energy in units of (Ryd/atom). The above equations show that the bulk modulus has large bowing parameters which emphasizes that the nonlinear

Table 4. The effect of 1D and 2D-search of EOS on the optimized values (volume, bulk modulus, derivate of bulk modulus (B') and energy) and pressure (P) of induced-phase transition of CdTe compound within PBE-GGA.

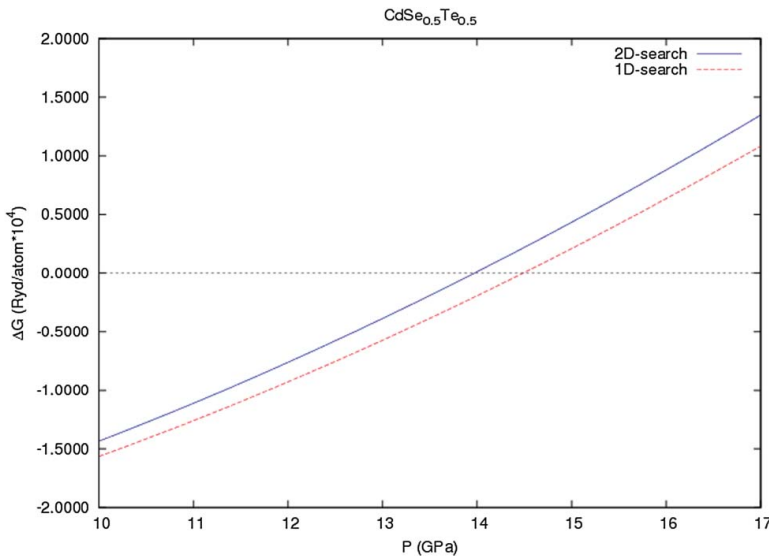
CdTe	V (bohr ³ /atom)	B (GPa)	B'	E (Ryd/atom)	P (GPa)
1D-search	245.6168	35.21	4.41	-12392.896945	11.4
2D-search	245.6107	35.25	4.36	-12392.896949	10.6

behavior of B against x changes as the bowing parameter of the cubic phase from linear fitting is bigger than that that for the wurtzite phase. While the a -lattice constant for the wurtzite phase deviates a little from the linearity as a function of x composition, the deviation from linearity for the cubic phase is bigger than that for the wurtzite phase. As can be seen from the above equations, the optimized volume for both phases behaves as nonlinear against x changes as the bowing parameter of the wurtzite phase from linearity is bigger than that for the cubic phase. While the optimized energy for the cubic phase deviates a little from the linearity as a function of x changes, the deviation from linearity for the wurtzite phase is bigger than that for the cubic phase.

3.2. Phase transition and stable phase

In the first step of this section and to show that the effect of 2D-search can be important for finding the pressure of induced phase transition, we have studied the ground-state properties of hexagonal CdTe and CdSe_{0.5}Te_{0.5} compounds using 2D-search of EOS. Our results (Table 4) show that the effect of 2D-search of EOS on the optimized values (E_0, V_0, B, B') for hexagonal phase of CdTe compound is negligible but these small changes lead the 2D-search of EOS to predict the pressure of induced phase transition be around 0.8 (GPa) lower than 1D-search of EOS for CdTe compound. Moreover, Figure 1 shows that 2D-search of EOS predicts the pressure of induced phase transition to be about 0.9 (GPa) lower than 1D-search of EOS for CdSe_{0.5}Te_{0.5} compound. Therefore, this effect (2D-search of EOS) can be important for finding the pressure of induced phase transition.

Figure 2(a) exhibits that the stable phase for CdSe compound is wurtzite which is in agreement with the previous prediction [17], while for ternary CdSe_{0.75}Te_{0.25}, CdSe_{0.5}Te_{0.5}, and CdSe_{0.25}Te_{0.75}

**Figure 1.** Difference of Gibbs free energy as function of pressure for two phases of CdSe_{0.5}Te_{0.5} compound within PBE – GGA using 2D and 1D-search of EOS for wurtzite phase.

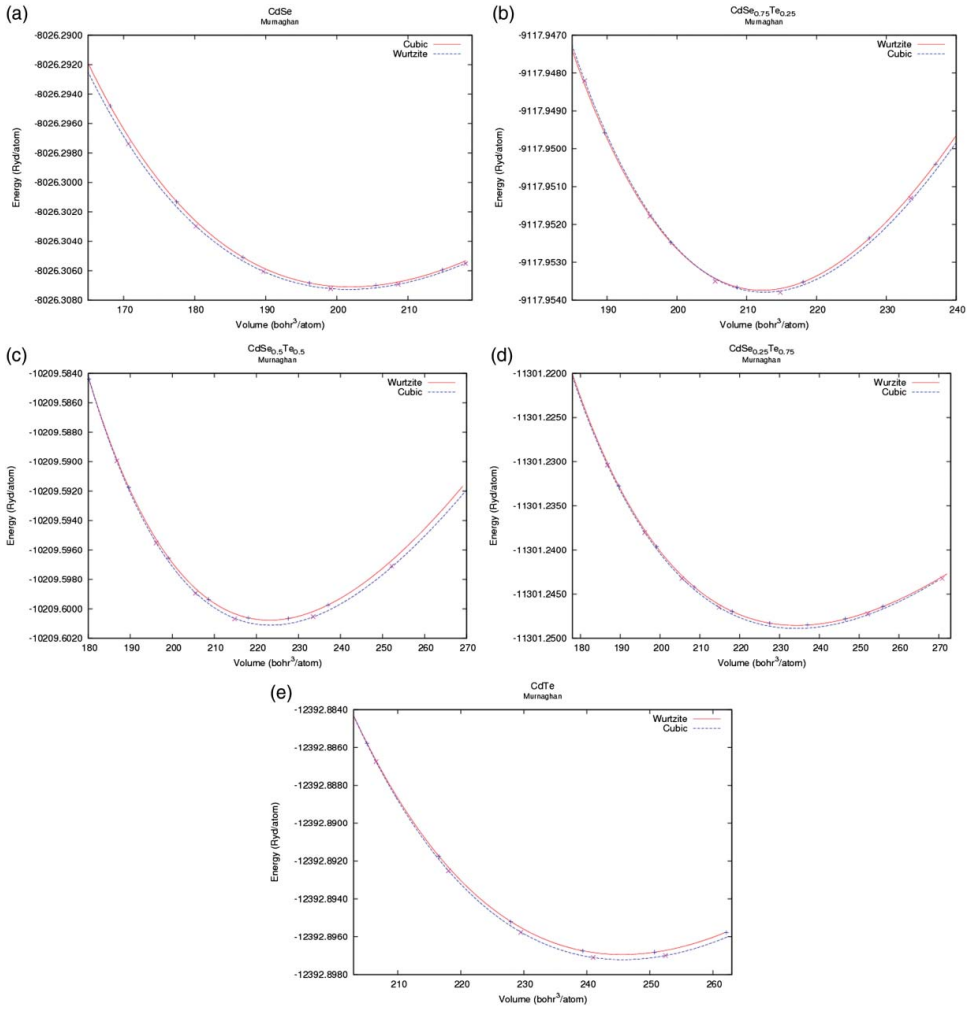


Figure 2. (a) Equation of state for two phases of CdSe compound within PBE – GGA. (b) Equation of state for two phases of CdSe_{0.75}Te_{0.25} compound within PBE – GGA. (c) Equation of state for two phases of CdSe_{0.5}Te_{0.5} compound within PBE – GGA. (d) Equation of state for two phases of CdSe_{0.25}Te_{0.75} compound within PBE – GGA. (e) Equation of state for two phases of CdTe compound within PBE – GGA.

alloys, the most stable phase is cubic as represented in Figure 2(b–d). These results are in agreement with the previous prediction [17] except for CdSe_{0.75}Te_{0.25}. Following Figure 2(e), it is found that CdTe compound is stable in the cubic phase that is consistent with the experimental work [50]. From our results at zero temperature ($T = 0$ K), we can predict for the range $0.25 \leq x \leq 1.0$, the bulk CdSe_{1-x}Te_x alloys exists (stable) in the cubic phase while for the range $0.0 \leq x < 0.25$, the stable phase is wurtzite. Schenk and Silber found that the cubic phase exists in the composition range $0 \leq x_{\text{CdSe}} \leq 0.45$, while the wurtzite phase in the range $0.65 \leq x_{\text{CdSe}} \leq 1.0$ for ternary CdSe_xTe_{1-x} alloys. Other experimental results show cubic structure for CdSe_xTe_{1-x} thin films in the whole composition range ($0 \leq x \leq 1$) [31–33], while in the new experimental work of Shinde et al. [11], the structure of the CdSe_{0.6}Te_{0.4} thin films was found to be hexagonal.

Using the obtained difference of Gibbs-free-energy ($\Delta G = 0$) at the same pressure grid, we are able to calculate the pressure-induced phase transition for two phases of CdSe_{1-x}Te_x alloys. Our

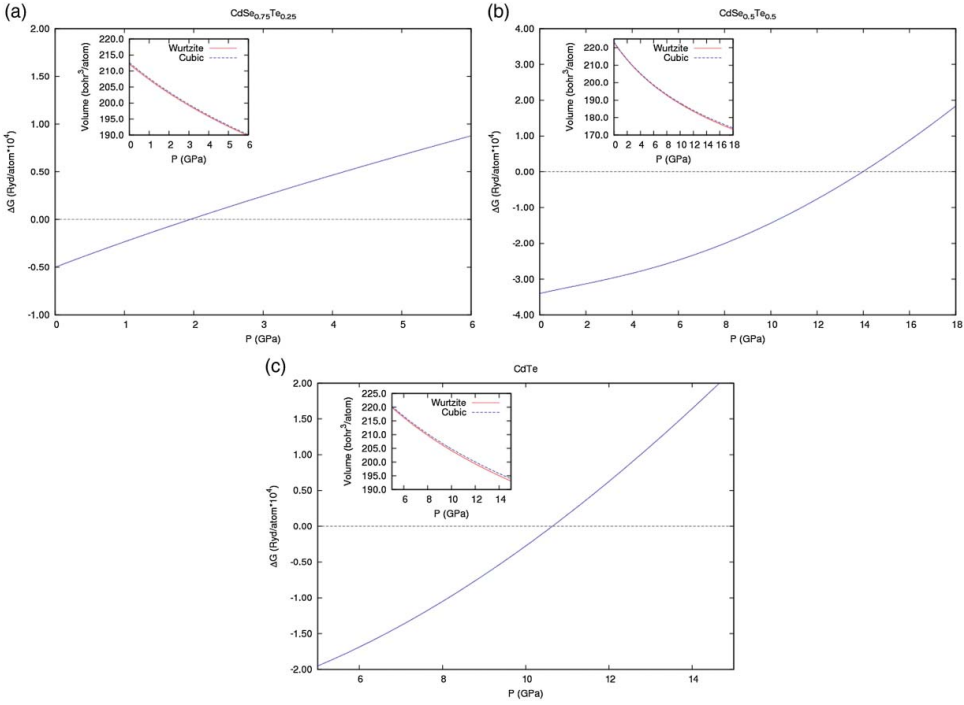


Figure 3. (a) Difference of Gibbs free energy as function of pressure for two phases of $\text{CdSe}_{0.75}\text{Te}_{0.25}$ compound within PBE – GGA. Inset: calculation of the volume versus pressure for two phases. (b) Difference of Gibbs free energy as a function of pressure for two phase of $\text{CdSe}_{0.5}\text{Te}_{0.5}$ compound within PBE – GGA. Inset: calculation of the volume versus pressure for two phases. (c) Difference of Gibbs free energy as function of pressure for two phases of CdTe compound within PBE – GGA. Inset: calculation of the volume versus pressure for two phases.

results show that DFT+PBE does not predict phase transition from wurtzite to cubic for CdSe compound at zero temperature. The same behavior is seen for $\text{CdSe}_{0.25}\text{Te}_{0.75}$ alloy. Therefore, we can conclude that a phase transition can occur in CdSe compound and $\text{CdSe}_{0.25}\text{Te}_{0.75}$ alloy at a temperature which is not equal to zero.

Following [Figure 3\(a\)](#), our results predict a possible pressure-induced phase transition from cubic to wurtzite phase for the ternary $\text{CdSe}_{0.75}\text{Te}_{0.25}$ alloy at a pressure of about 1.9 (GPa) using 2D and 1D search of EOS. The corresponding volume collapses at the phase-transition boundary are also calculated to be 203.839 and 203.485 and 203.839 and 203.489 ($\text{bohr}^3/\text{atom}$) using 2D and 1D search of EOS, respectively, while [Figure 3\(b\)](#) indicates a possible pressure-induced phase transition from cubic to wurtzite phase for the ternary $\text{CdSe}_{0.5}\text{Te}_{0.5}$ alloy at pressure of about 13.6 and 14.5 (GPa) using 2D and 1D search of EOS, respectively. The corresponding volume collapses at the phase-transition boundary are also calculated to be 181.115 and 180.525 and 179.532 and 178.940 ($\text{bohr}^3/\text{atom}$) using 2D and 1D search of EOS, respectively. Also, we found that (see [Figure 3\(c\)](#)) the DFT+PBE calculation predicts phase transition from cubic to wurtzite for CdTe compound at pressure of about 10.6 and 11.4 (GPa) using 2D and 1D search of EOS, respectively. The corresponding volume collapses at the phase-transition boundary are also calculated to be 203.337 and 202.692 and 201.433 and 200.861 ($\text{bohr}^3/\text{atom}$) using 2D and 1D search of EOS, respectively. Thus, we can predict that for the compositions between $0.25 \leq x \leq 0.5$ and $x = 1.0$ at zero temperature, a phase transition may occur depending on pressure treatment for ternary $\text{CdSe}_{1-x}\text{Te}_x$ alloys. The corresponding lattice parameter collapses at the phase-transition boundary were also calculated using 2D and 1D search of EOS as listed in [Table 5](#).

Table 5. The calculated lattice-parameters (a and c in bohr) at the pressure (P in GPa) of induced-phase transition within PBE-GGA.

Compounds	P (GPa)	a (Bohr)	c (Bohr)
CdTe _{cubic}	11.4	11.7608	
CdTe _{wurtzite(1D)}	11.4	8.2956	13.6040
CdTe _{cubic}	10.6	11.7240	
CdTe _{wurtzite(2D)}	10.6	8.2796	13.5335
CdSe _{0.5} Te _{0.5} cubic	14.5	11.2826	
CdSe _{0.5} Te _{0.5} wurtzite(1D)	14.5	7.9700	13.0114
CdSe _{0.5} Te _{0.5} cubic	13.6	11.2157	
CdSe _{0.5} Te _{0.5} wurtzite(2D)	13.6	7.9880	13.0675
CdSe _{0.75} Te _{0.25} cubic	1.9	11.7704	
CdSe _{0.75} Te _{0.25} wurtzite(1D)	1.9	8.3189	27.1622
CdSe _{0.75} Te _{0.25} cubic	1.9	11.7704	
CdSe _{0.75} Te _{0.25} wurtzite(2D)	1.9	8.3176	27.1703

4. Conclusions

The SQS approach of Zunger et al. is used to reproduce the randomness of the CdSe_{1-x}Te_x ($x = 0.0, 0.25, 0.5, 0.75, 1.0$) alloys for the first few shells around a given site. The all-electron full potential linearized augmented plane wave (FP-LAPW) method was used to calculate pressure-induced phase transition at zero temperature for selected phases at the same pressure grid. Therefore, we have investigated the ground-state properties of CdSe_{1-x}Te_x alloys in the cubic and wurtzite phases. Calculations show that CdSe is stable at wurtzite phase, while for ternary CdSe_{0.75}Te_{0.25}, CdSe_{0.5}Te_{0.5}, CdSe_{0.25}Te_{0.75} and CdTe, the most stable phase is cubic. From our results at zero temperature, we can predict for the range $0.25 \leq x \leq 1.0$ that the CdSe_{1-x}Te_x alloy exists (stable) in the cubic phase, while for the range $0.0 \leq x < 0.25$, the stable phase is wurtzite. This prediction is consistent with experimental work of Schenk and Silber at $T < 800$ °C except for CdSe_{0.75}Te_{0.25}. We found that increasing the Te content in the cubic phase of ternary CdSe_{1-x}Te_x alloys causes to decrease, increase, and decrease the optimized energy, volume, and bulk modulus, respectively, whereas for the wurtzite phase of the ternary CdSe_{1-x}Te_x alloys, increasing the Te content causes to increase the optimized volume and decrease the energy and bulk modulus, and hence leads to decrease the resistance against the volume changes (hardness) for both phases. We found that the DFT+PBE calculation predicts phase transition from cubic to wurtzite for CdTe compound at pressure of about 10.6 and 11.4 (GPa) using 2D and 1D search of EOS, respectively. The corresponding volume collapses at the phase-transition boundary are also calculated to be 203.337 and 202.692 and 201.433 and 200.861 (bohr³/atom) using 2D and 1D search of EOS, respectively.

Also, the DFT calculation within PBE – GGA predicts a possible pressure-induced phase transition from cubic to wurtzite phase for the ternary CdSe_{0.5}Te_{0.5} alloy at pressure of about 13.6 and 14.5 (GPa) using 2D and 1D search of EOS, respectively. The corresponding volume collapses at the phase-transition boundary were also calculated as 181.115 and 180.525 and 179.532 and 178.940 (bohr³/atom) using 2D and 1D search of EOS, respectively. Moreover, a possible pressure-induced phase transition is indicated from cubic to wurtzite phase for the ternary CdSe_{0.75}Te_{0.25} alloy at a pressure of about 1.9 (GPa) using 2D and 1D search of EOS. The corresponding volume collapses at the phase-transition boundary are also calculated to be 203.839 and 203.485 and 203.839 and 203.489 (bohr³/atom) using 2D and 1D search of EOS, respectively.

Disclosure statement

No potential conflict of interest was reported by the authors.

Funding

The result was developed within the CENTEM project [reg. no. CZ.1.05/2.1.00/03.0088], cofunded by the ERDF as part of the Ministry of Education, Youth and Sports OP RDI programme and, in the follow-up sustainability stage, supported through CENTEM PLUS [LO1402] by financial means from the Ministry of Education, Youth and Sports

under the National Sustainability Programme I. Computational resources were provided by MetaCentrum [LM2010005] and CERIT-SC [CZ.1.05/3.2.00/08.0144] infrastructures.

References

- [1] Hurwitz CE. Electron-beam pumped lasers of CdSe and CdS. *Appl Phys Lett*. 1966;8:121–124.
- [2] Nicoll FH. Ultraviolet ZnO laser pumped by an electron beam. *Appl Phys Lett*. 1966;9:13–15.
- [3] Bailey RE, Strausburg JB, Nie S. A new class of far-red and near-infrared biological labels based on alloyed semiconductor quantum dots. *J Nanosci Nanotechnol*. 2004;4:569–574.
- [4] More PD, Shahane GS, Deshmukh LP, et al. Spectro-structural characterisation of CdSe_{1-x}Te_x alloyed thin films. *Mater Chem Phys*. 2003;80:48–54.
- [5] Azhniuk Y, Hutyck YI, Lopushansky VV, et al. Phonon spectroscopy of CdSe_{1-x}Te_x nanocrystals grown in a borosilicate glass. *Phys Status Solidi (c)*. 2009;6(9):2064–2067.
- [6] Konstantinova-Kabassanova E, Nenova Z, Lusson A, et al. Large grain CdSe_{0.9}Te_{0.1} layers grown from the vapor in presence of α -Cr₂O₃. *J Mater Sci: Mater Electron*. 2000;11:679–683.
- [7] Wei S, Zhang SB. Structure stability and carrier localization in CdX(X = S,Se,Te) semiconductors. *Phys Rev B*. 2000;62:6944–6947.
- [8] El-Sayed SM. The study of dielectric relaxation and glass forming tendency in Cd–Se–Te glassy system. *Appl Surf Sci*. 2007;253:7089–7093.
- [9] Sathyamoorthy R, Sudhagar P, Kumar RS, et al. Facile synthesis of thiol-stabilized CdSe_xTe_{1-x} nanocrystals. *Physica B*. 2011;406:715–719.
- [10] Shinde SK, Thombare JV, Dubal DP, et al. Electrochemical synthesis of photosensitive nano-nest like CdSe_{0.6}Te_{0.4} thin films. *Appl Surf Sci*. 2013;282:561.
- [11] Shinde SK, Dubal DP, Ghodake GS, et al. Synthesis and characterization of chemically deposited flower-like CdSe_{0.6}Te_{0.4} thin films for solar cell application. *Mater Lett*. 2014;126:17–19.
- [12] Shinde SK, Ghodake GS, Dubal DP, et al. Structural, optical, and photo-electrochemical properties of marygold-like CdSe_{0.6}Te_{0.4} synthesized by electrochemical route. *Ceram Int*. 2014;40:11519–11524.
- [13] Merad AE, Kanoun MB, Merad G, et al. Full-potential investigation of the electronic and optical properties of stressed CdTe and ZnTe. *Mater Chem Phys*. 2005;92:333–339.
- [14] Benyettou S, Saib S, Bouarissa N. Elastic, lattice dynamical and thermal properties of zinc-blende CdSe_xTe_{1-x} ternary alloys. *Chem Phys*. 2015;457:147–151.
- [15] Saib S, Benyettou S, Bouarissa N, et al. First principles study of structural, elastic and piezoelectric properties of CdSe_xTe_{1-x} ternary alloys in the wurtzite structure. *Phys Scr*. 2015;90:035702.
- [16] Jamal M, Abu-Jafar MS, Reshak AH. Revealing the structural, elastic and thermodynamic properties of CdSe_xTe_{1-x} ($x = 0, 0.25, 0.5, 0.75, 1$). *J Alloys Compd*. 2016;667:151–157.
- [17] Reshak AH, Kityk IV, Khenata R, et al. Effect of increasing tellurium content on the electronic and optical properties of cadmium selenide telluride alloys CdSe_{1-x}Te_x: an *ab initio* study. *J Alloys Compd*. 2011;509:6737–6750.
- [18] Das VD. Thin film photoelectrodes of ternary chalcogenide CdSe_{1-x}Te_x for photoelectrochemical solar cells applications. In: Gopalam BSV, Majhi Madras J, editors. Conference on Physics and Technology of semiconductor devices and integrated circuits. Proceedings of SPIE; 1992 Feb 1; India. Vol. 1523. p. 326.
- [19] Bhattacharya C, Datta J. Synthesis of nanostructured Cd–Se–Te films through periodic voltammetry for photo-electrochemical applications. *J Solid State Electrochem*. 2007;11:215–222.
- [20] Matsumura N, Sakamoto T, Saraie J. Growth conditions in molecular beam epitaxy for controlling CdSeTe epilayer composition. *J Cryst Growth*. 2003;251:602–606.
- [21] Ravichandran D, Xavier FP, Sasikala S, et al. Photoconductivity studies of CdSe_{1-x}Te_x thin films as a function of doping concentration. *Bull Mater Sci*. 1996;19:437–442.
- [22] Muthukumarasamy N, Jayakumar S, Kannan MD, et al. Structural phase change and optical band gap bowing in hot wall deposited CdSe_xTe_{1-x} thin film. *Solar Energy*. 2009;83:522–526.
- [23] Ouendadji S, Ghemid S, Meradji H, et al. Density functional study of CdS_{1-x}Se_x and CdS_{1-x}Te_x alloys. *Comput Mater Sci*. 2010;48:206–211.
- [24] Schenk M, Silber C. Lattice parameter and microhardness investigations on CdTe_{1-x}Se_x. *J Mater Sci: Mater Electron*. 1998;9:295–300.
- [25] Uthanna S, Jayarama Reddy P. Structural and electrical properties of CdSe_xTe_{1-x} thin films. *Solid State Commun*. 1983;45:979–980.
- [26] Mangalharu JP, Thangaraj R, Agnihotri OP. Structural, optical and photoluminescence properties of electron beam evaporated CdSe_{1-x}Te_x films. *Sol Energy Mater*. 1989;19:157–165.
- [27] Islam R, Banerjee HD, Rao DR. Structural and optical properties of CdSe_xTe_{1-x} thin films grown by electron beam evaporation. *Thin Solid Film*. 1995;266:215–218.
- [28] Webb AW, Qadri SB, Carpenter ER Jr, et al. Effects of pressure on Cd_{1-x}Zn_xTe alloys ($0 < x < 0.5$). *J Appl Phys*. 1987;61:2492–2494.

- [29] Adachi S. Handbook on physical properties of semiconductors: II–VI semiconductors. Vol. 3. Boston (MA): Kluwer Academic; 2004.
- [30] Vnuk F, Monte AD, Smith RW. The effect of pressure on the semiconductor-to-metal transition temperature in tin and in dilute tin-germanium alloys. *J Appl Phys.* 1984;55:4171–4176.
- [31] Liu CY, Spain IL, Skelton EF. Study of the pressure-induced structural phase transition in the $Ga_{(1-x)}In_xSb$ alloy system. *J Phys Chem Solids.* 1987;39:113–122.
- [32] Béliveau A, Carbone C. Influence of concentration on the structural-phase-transition pressure of the II–VI ternary alloy $Zn_xCd_{1-x}S$. *Phys Rev B.* 1991;44:3650–3654.
- [33] Tiong SR, Hiramatsu M, Matsushima Y, et al. The phase transition pressures of zinc sulfoselenide single crystals. *Jpn J Appl Phys.* 1989;28:291.
- [34] Pellicer-Porres J, Martínez-García D, Ferrer-Roca C, et al. High-pressure phase diagram of $ZnSe_xTe_{1-x}$ alloys. *Phys Rev B.* 2005;71:035210–035216.
- [35] Adachi S. Properties of semiconductor alloys: group-IV, III–V and II–VI semiconductors. West Sussex: Wiley; 2009.
- [36] Madsen GKH, Blaha P, Schwarz K, et al. Efficient linearization of the augmented plane-wave method. *Phys Rev B.* 2001;64:195134–195142.
- [37] Schwarz K, Blaha P, Madsen GKH. Electronic structure calculations of solids using the WIEN2k package for material sciences. *Comput Phys Commun.* 2002;147:71–76.
- [38] Blaha P, Schwarz K, Madsen GKH, et al. Computer code WIEN2k, an augmented plane wave plus local orbitals program for calculating crystal properties. Vienna: Vienna University of Technology; 2001. ISBN 3-9501031-1-2.
- [39] 2DROptimize package is provided by M. Jamal as part of the commercial code WIEN2K. Available from: <http://www.wien2k.at>
- [40] Reshak AH, Jamal M. Calculation of the lattice constant of hexagonal compounds with two dimensional search of equation of state and with semilocal functionals a new package (*2D-optimize*). *J Alloys Compd.* 2013;555:362–366.
- [41] Jamal M, Asadabadi SJ, Ahmad I, et al. Elastic constants of cubic crystals. *Comput Mater Sci.* 2014;95:592–599.
- [42] Reshak AH, Jamal M. DFT calculation for elastic constants of orthorhombic structure within WIEN2K code: a new package (*ortho-elastic*). *J Alloys Compd.* 2012;543:147–151.
- [43] Jamal M, KamaliSarvestani N, Yazdani A, et al. Mechanical and thermodynamical properties of hexagonal compounds at optimized lattice parameters from two-dimensional search of the equation of state. *RSC Adv.* 2014;4:57903–57915.
- [44] Haas P, Tran F, Blaha P. Calculation of the lattice constant of solids with semilocal functionals. *Phys Rev B.* 2009;79:085104–085113.
- [45] Perdew JP, Burke K, Ernzerhof M. Generalized gradient approximation made simple. *Phys Rev Lett.* 1996;77:3865–3868.
- [46] Zunger A, Wei S-H, Feireira LG, et al. Special quasirandom structures. *Phys Rev Lett.* 1990;65:353–356.
- [47] Huang M-Z, Ching WY. Calculation of optical excitations in cubic semiconductors. I. Electronic structure and linear response. *Phys Rev B.* 1993;47:9449–9463.
- [48] Mangalhara JP, Thangaraj R, Agnihotrii OP. Structural, optical and photoluminescence properties of electron beam evaporated $CdSe_{1-x}Te_x$ films. *Solar Energy Mater.* 1989;19:157–165.
- [49] Madelung O, Schlz M, Weiss H. Landolt–Borstein: numerical data and functional relationships in science and technology. Vol. 17. Berlin: Springer; 1982.
- [50] Hosseini SM. Optical properties of cadmium telluride in zinc-blende and wurzite structure. *Physica B.* 2008;403:1907–1915.
- [51] Wyckoff RWG, editor. Crystal structures. Vol. 1. New York: Wiley; 1963.
- [52] Heyd J, Peralta JE, Scuseria GE. Energy band gaps and lattice parameters evaluated with the Heyd–Scuseria–Ernzerhof screened hybrid functional. *J Chem Phys.* 2005;123:174101.
- [53] Deligoz E, Colakoglu K, Ciftci Y. Elastic, electronic, and lattice dynamical properties of CdS, CdSe, and CdTe. *Physica B.* 2006;373:124–130.
- [54] Zerroug S, Ali Sahraoui F, Bouarissa N. Structural parameters and pressure coefficients for CdS_xTe_{1-x} : FP-LAPW calculations. *Eur Phys J B.* 2007;57:9–14.